

Influence of annealing temperature and atmosphere on surface microstructure and magnetism in FINEMET-type FeSiNbCuB ribbons

Ondřej Životský¹, Yvonna Jirásková², Aleš Hendrych¹, Vlastimil Matějka³, Ladislav Klimša¹, and Jiří Buršík²

¹Institute of Physics, VŠB-Technical University of Ostrava, Ostrava, CZ 70833, Czech Republic

²Institute of Physics of Materials, Academy of Sciences of the Czech Republic, Brno, CZ 61662, Czech Republic

³Nanotechnology Centre, VŠB-Technical University of Ostrava, Ostrava, CZ 70833, Czech Republic

Paper is primarily devoted to the surface investigations of the FINEMET-type $\text{Fe}_{73.5}\text{Si}_{13.5}\text{Nb}_3\text{Cu}_1\text{B}_9$ ribbons. As-quenched (AQ) samples were subsequently annealed at different temperatures from 733 K to 923 K in vacuum and hydrogen in order to follow the influence of both treatment parameters on microstructure and magnetic properties. Two-phase magneto-optical (MO) hysteresis loops observed at AQ ribbons correspond to an amorphous structure composed of clusters of the size in units of nm (calculated from XRD). The annealing temperatures are responsible for the origin of the α -Fe and/or α -Fe(Si) nanocrystals of various size formed at the surface and consequently penetrating into the ribbon volume while the atmospheres influence surface oxidation. An interesting occurrence of the asymmetric reversal of longitudinal magnetization, clearly observed after annealing at 733 K and 743 K, is discussed from the viewpoint of quadratic magneto-optical effects. The loop asymmetry decreases with increasing annealing temperature and disappears at 923 K.

Index Terms— Soft magnetic materials, nanostructured materials, quadratic magneto-optical effects, magnetic domains, X-ray scattering, electron microscopy

I. INTRODUCTION

AMORPHOUS and nanocrystalline alloys in the form of the ribbons are investigated mainly due to their excellent soft magnetic properties [1]. It is generally known that decrease of volume coercive field and increase of saturation magnetic moment are closely related to the temperature treatment of these alloys. The as-quenched state embodies mostly amorphous structure with a certain local ordering of atoms into clusters [2]. The subsequent annealing causes rearrangement of the clusters and their additional transformation into the form of nanocrystals starting from the surface. This process is affected also by annealing atmosphere. Treatment mechanisms together with change of addition elements in the alloy compositions are often used for tuning the size of grains and penetration depth of nanocrystals at the expense of amorphous bulk [3, 4].

Recently, increasing interest in the surface magnetic and microstructure properties of these materials is connected with development of sensors working in GHz range [5]. Behavior of amorphous clusters (nanoscale phase separation) and nanocrystals as the key parameters for correct function of the system have been investigated by various surface-sensitive methods [6-9]. Their combination is necessary for understanding the surface processes originating during planar flow casting and subsequent treatment of the ribbons.

Present work is focused on the surface magnetic properties of FINEMET-type $\text{Fe}_{73.5}\text{Si}_{13.5}\text{Nb}_3\text{Cu}_1\text{B}_9$ ribbons that have been studied in the as-quenched (AQ) state and after annealing at 733 K, 743 K, 823 K, and 923 K in vacuum and hydrogen. For both atmospheres an interesting magnetization behavior, manifested by antisymmetric hysteresis loops, has been detected. Our elucidation is based on the quadratic magneto-

optical Kerr effect (QMOKE) [10, 11] that has never been observed in these alloys. Gradual vanishing of QMOKE with increasing annealing temperature adverts to strong correlation with the surface microstructure. Simultaneous investigations using X-ray diffraction (XRD), grazing incident XRD (GIXRD), and transmission electron microscopy provide unique insight into the process of surface nanocrystallization in both atmospheres.

II. EXPERIMENTAL

$\text{Fe}_{73.5}\text{Si}_{13.5}\text{Nb}_3\text{Cu}_1\text{B}_9$ alloy in the form of about 20 μm thick and 6 mm wide ribbon was prepared by planar flow casting method. Samples were additionally annealed for 1h at temperatures (T_a) of 733 K, 743 K, 823 K, and 923 K in vacuum (10^{-5}Pa) and hydrogen atmospheres. At all experiments the shiny ribbon side, i.e. side in contact with the air during quenching process, was investigated. The reason is that side in contact with the wheel (wheel side) exhibits higher surface roughness that usually excludes possibility of used optical methods to characterize surface without additional treatment.

Surface magnetic properties were studied using the methods based on magneto-optical Kerr effect (MOKE). Hysteresis loops obtained from the surface area of tens of nanometers (for pure Fe at wavelength of 670 nm the penetration depth is about 16 nm [12]) describe the reversal of longitudinal magnetization component M_L lying in the sample plane and plane of incidence of light. Magneto-optical angle of Kerr rotation was measured as a function of external magnetic field that is parallel to M_L and to the original ribbon axis. No polar (out-of-plane) magnetization component has been observed. S-polarized red light ($\lambda = 670\text{ nm}$) with beam diameter about 300 μm incidents the sample surface at the angle of 50°. In order to check the homogeneity of the samples and influence of surface roughness laser spot was focused in different places

Manuscript received January 1, 2011. Corresponding author: O. Životský (e-mail: ondrej.zivotsky@post.cz). Digital Object Identifier inserted by IEEE

on the ribbon surface. Magneto-optical measurements are supplemented by observations of surface magnetic domains using the MO Kerr microscopy.

The microstructure and composition of samples were checked by the XRD and GIXRD. Standard XRD spectra obtained using $\text{CoK}\alpha$ radiation in Bragg-Brentano geometry yield information from penetration depth about $10\text{ }\mu\text{m}$. For correlations with MOKE detected area the lamp was fixed at grazing angle of 1.5° to scan the properties from the surface region lower than 100 nm . In order to complement the XRD results the subsurface microstructure of two selected samples was investigated by means of transmission electron microscopy (TEM) using a Philips CM12 STEM microscope with acceleration voltage 120 kV . Samples for TEM were prepared in a form of thin lamellas (lateral dimensions about $10\times 8\text{ }\mu\text{m}$) perpendicular to the shiny ribbon side using focused ion beam (FIB) technique in a TESCAN LYRA 3 XMU FEG/SEM×FIB scanning electron microscope.

III. EXPERIMENTAL RESULTS

A. Microstructure

The XRD measurement of the AQ sample has pointed out an amorphous structure in agreement with TEM micrograph (Fig. 1a) revealing almost featureless microstructure with contrast fluctuations of the size below $1\text{--}2\text{ nm}$. Corresponding selected area diffraction (SAD) pattern (Fig. 1b) shows a diffuse ring typical of amorphous materials.

Fig. 2 represents the XRD patterns of samples annealed in vacuum (left column) and hydrogen (right column). The sharp crystalline peak, superimposed on the broader amorphous halo, corresponds to the bcc-FeSi phase as obtained from Rietveld analysis [13]. It is seen only on patterns of samples annealed in vacuum at lower T_a . The FeSi content gradually grows with increasing T_a (from 8 % at 733 K to 40 % at 823 K). The grain size varies between 10 and 13 nm . On the other hand the samples, annealed in hydrogen at 733 K and 743 K , are amorphous with the size of coherent domains (clusters) about 2 nm . Presence of crystalline bcc-FeSi phase is visible as late as at 823 K (content about 50 %). The nanocrystal size of these samples ($10\div 15\text{ nm}$) is optimal for obtaining the excellent soft magnetic properties (H_c not higher than 4 Oe , well comparable with volume coercivity obtained using vibrating sample magnetometer). Its increase after annealing at 923 K (not shown here) to about $(40\div 50)\text{ nm}$ and the origin of FeB crystalline phases (XRD) contribute to a strong deterioration of magnetic softness.

Results of GIXRD measurements at $T_a = 733\text{ K}$ and 823 K in vacuum and hydrogen are shown in Fig. 3. Detected peaks approve the surface crystallization also in the sample annealed at 733 K in hydrogen. The Rietveld analysis of all patterns has yielded the crystalline $\alpha\text{-Fe}$ phase or $\alpha\text{-Fe}$ with small amount of Si (below 1 at.%), formation of B_2O on samples annealed in both atmospheres, and of FeBO_3 after annealing in vacuum. Presence of small amorphous halo is seen on the samples annealed at 733 K only. The surface oxidation strongly depends on annealing atmosphere as follows from Table 1. While hydrogen seems to inhibit the surface oxidation, vacuum of 10^{-5} Pa contains enough oxygen to form B_2O

and/or FeBO_3 . The size of $\alpha\text{-Fe}$ and/or $\alpha\text{-Fe(Si)}$ nanocrystals between 5 nm (733 K) and 13 nm (823 K) was calculated using Rietveld procedure of GIXRD patterns.

TEM study of vacuum-annealed sample at 743 K (Fig. 1c) reveals distinct nanocrystals (the dark ones in the bright field electron micrograph fulfil the diffraction condition) with size about $5\text{--}15\text{ nm}$. Corresponding SAD pattern (Fig. 1d) shows sharp dense rings typical of ultra fine grain material. All the rings index as bcc structure with lattice parameter about 0.28 nm . A weak diffuse ring of amorphous phase was found at the background of sharp rings.

B. Surface magneto-optical properties

Fig. 4 shows the results of MOKE hysteresis loops obtained on the AQ and annealed samples at both annealing atmospheres. From the hysteresis loop of the AQ ribbon it is clearly seen that it consists of two overlapped minor loops detecting two magnetically different phases in the near-surface region. Change of the loop shape, when the light is focused into the different places, is attributed to the strong inhomogeneous magnetic behavior. This is connected with random clusters anisotropy influenced by internal stress relief. The stresses, originating from the preparation process and being responsible for magnetic inhomogeneities, influence the domain structure and are shown in Fig. 5. Wide-curved domains visible on the AQ sample (Fig. 5a) are the consequence of tensile stress, while the regions characterized by the fingerprint-like domains were exposed to the planar compressive stress.

The annealing at 733 K (Fig. 5b) and consequently also at 743 K contribute to relaxation of stresses. The fingerprint domains almost completely disappear and the increasing width of planar domains indicates a preference of magnetization direction in the ribbon plane as well as at the sample after annealing at 823 K (Fig. 5c). On the other hand an asymmetric magnetization reversal is observed in both atmospheres (second row of Fig. 4). An origin of this phenomenon can be explained using the quadratic magneto-optical Kerr effects (QMOKE) discussed in the next section. Further increase of T_a results in marked decrease of QMOKE amplitudes. It is documented by the third row of Fig. 4 showing the loops measured on samples annealed at 823 K . QMOKE has fully disappeared after annealing at 923 K .

IV. DISCUSSION

The amorphous state of the AQ sample was independently confirmed by XRD, TEM (Fig. 1a, b), and by conversion electron Mössbauer spectroscopy (not presented here). Nevertheless the MOKE results show a presence of two magnetically different components. Similarly as in the case of FeSiB alloys [12], MOKE redisplay the amorphous structure ordered into chemically different clusters with slightly dissimilar magnetic behavior. Because Kerr microscopy was not able to detect them, their size has to be under the limit of its optical resolution, which means in units of nm as was calculated from XRD. On the other hand the Kerr microscopy has yielded magnetically inhomogeneous surface by the presence of wide-curve and fingerprint-like domains as a consequence of stress relief mentioned above.

The results obtained on annealed samples revealed an asymmetry in magnetization reversal that was the largest at samples annealed at 733 K in both atmospheres. Up to now such asymmetry was observed at thin-film systems only. The GIXRD measurements have detected almost crystallized close surface regions (approx. thickness of 100 nm) with an insignificant presence of an amorphous phase namely at the vacuum annealed sample. Therefore such relatively large asymmetry could not come from exchange bias between nanocrystals and amorphous matrix and we have made a hypothesis that measured asymmetric hysteresis loops are the consequence of quadratic magneto-optical effects. They exhibit an even dependence on the applied magnetic field and are superimposed on the first order linear contributions (M_L in our case). Although the symmetry conditions enable to observe QMOKE in arbitrary structure, practical preparation of such materials is rather complicated. Till now huge contributions of QMOKE have been experimentally detected and described only in several well-defined bcc structures like Fe/MgO [10] or Co₂-based Heusler compounds [11].

An origin of QMOKE in present studies can be attributed to the very small α -Fe and/or α -Fe(Si) nanocrystals dispersed in oxides as detected by GIXRD. Random orientation of nanocrystals explains the fact why the size of QMOKE is changing, when the light is focused into the different places on the ribbon surface. It is known that each measured magneto-optical hysteresis loop can be divided into symmetric part containing odd linear effects and antisymmetric part with even quadratic effects [11]. Examples of separated QMOKE from loops at 733 K are shown in insets of the second row of Fig. 4. Because no polar magnetization component is present, signal corresponding to quadratic effects is proportional to the mixed terms of $M_L M_T$ and $M_L^2 - M_T^2$, where M_T is transversal in-plane magnetization component perpendicular to the plane of incidence. Our measurements using the method, when external magnetic field is applied in eight directions without rotation of the sample [11], confirm the existence of both components with prevailing contribution of $M_L M_T$ term. It must be stressed that this method uses the effects in saturation. Therefore it is not influenced by the strong shape anisotropy of soft magnetic materials if an applied magnetic field saturates the sample in all directions.

The annealing at 743 K and namely at 823 K has evoked changes at the surface (Table 1) as well as in the bulk (Fig. 2) that are probably responsible for gradual symmetrization of the loops. Nevertheless some measured loops still exhibit a certain degree of asymmetry reflected in visible QMOKE indicating the inhomogeneous surface nanocrystallization. QMOKE disappears at samples annealed at 923 K. Entire loop symmetry and marked increase in coercivity to about 100 Oe and 20 Oe for vacuum and hydrogen atmospheres, respectively, are connected with the strong surface crystallization. XRD patterns analysis yielded presence of α -Fe(Si) with the grain size of about 50 nm and, moreover, boride phases. This is reflected also on the images of magnetic domains (Fig. 5d).

V. CONCLUSIONS

The relatively frequently studied FINEMET type alloy in a ribbon form was subjected in the present paper predominantly to the surface investigations. The asymmetric reversal of longitudinal magnetization in the alloy prepared by planar flow casting process was observed for the first time. This is a new phenomenon discussed from the viewpoint of quadratic magneto-optical effects. Deeper understanding of this effect can bring some new aspects important for the sensor applications of this material.

ACKNOWLEDGMENT

We thank to Dr. Dušan Janičkovič for preparation of the samples and to Dr. Jaroslav Hamrle for discussions devoted to quadratic magneto-optical effects. This work has been partially supported by the grants MSM6198910016, SP2011/26, CZ.1.05/2.1.00/01.0040, P205/11/2137 at IP TU, by 1M6198959201, AV0Z20410507 and by P108/11/1350 at IPM.

REFERENCES

- [1] A. Inoue, K. Hashimoto, *Amorphous and nano-crystalline materials*, 1st ed., vol. 3. Springer, 2001, pp. 1-216.
- [2] A. Chrobak, V. Nosenko, G. Haneczok, L. Boichyshyn, B. Kotur, A. Bajorek, O. Zivotsky, A. Hendrych, "Effect of rare earth additions on magnetic properties of Fe₈₂Nb₂B₁₄RE₂ (RE = Y, Gd, Tb and Dy) amorphous alloys," *Mat. Chem. Phys.*, to be published (doi: 10.1016/j.matchemphys.2011.07.031).
- [3] Y.Y. Jia, Z. Wang, R-M. Shi, J. Yang, H-J. Kang, T. Lin, "Influence of Ni addition on structure and magnetic properties of FeCo-based Finemet-type alloys," *J. Appl. Phys.* New York, vol. 109, pp. 073917, April 2011.
- [4] D-T. Ngo, M. S. Mahmud, H-H. Nguyen, H-G. Duong, Q-H. Nguyen, S. McVitie, Ch. Nguyen, "Crystallisation progress in Si-rich ultra-soft nanocomposite alloy fabricated by melt spinning," *J. Magn. Magn. Mater.* Amsterdam, vol. 322, pp. 342-347, February 2010.
- [5] Y. X. Wang, G. N. Zhao, B. Yan, H. Y. Wang, W. Lu, and Y. Zhang, "Structural evolution mechanism of early-stage nanocrystallization of Finemet amorphous ribbons," *IEEE Trans. Appl. Supercon.* New York, vol. 20, pp. 1638-1641, June 2010.
- [6] A. Chrobak, G. Haneczok, G. Chelkowska, L. Madej, "Effect of structural disorder on magnetic frustration in the Fe₈₀Nb₆B₁₄ amorphous alloy," *J. Magn. Magn. Mater.* Amsterdam, vol. 322, pp. 1105-1108, June 2010.
- [7] M. Aykol, A.O. Mekhrabov, M.V. Akdeniz, "Nano-scale phase separation in amorphous Fe-B alloys: Atomic and cluster ordering," *Acta Materialia*. Amsterdam, vol. 57, pp. 171-181, January 2009.
- [8] K. Kristiakova, P. Svec, "Continuous distribution of thermodynamic microprocesses in complex metastable systems," *Phys. Rev. B. USA*, vol. 64, pp. 184202, November 2001.
- [9] S.P. Chenakin, G.G. Galstyan, A.B. Tolstogousov, N. Kruse, "XPS and ToF-SIMS characterization of a Finemet surface: effect of heating," *Surf. Interf. Anal.* England, vol. 41, pp. 231-237, March 2009.
- [10] K. Postava, H. Jaffres, A. Schuhl, F. Nguyen Van Dau, M. Goiran, A.R. Fert, "Linear and quadratic magneto-optical measurements of the spin reorientation in epitaxial Fe films on MgO," *J. Magn. Magn. Mater.* Amsterdam, vol. 172, pp. 199-208, August 1997.
- [11] J. Hamrle, S. Blomeier, O. Gaier, B. Hillebrands, H. Schneider, G. Jakob, K. Postava, C. Felser, "Huge quadratic magneto-optical Kerr effect and magnetization reversal in the Co₂FeSi Heusler compound," *J. Phys. D: Appl. Phys.* Bristol, vol. 40, pp. 1563-1569, March 2007.
- [12] O. Zivotsky, Y. Jiraskova, A. Hendrych, J.M. Gomez, J. Bursik, L. Klimsa, D. Janickovic, "Surface microstructure and magnetic behavior in FeSiB amorphous ribbons from magneto-optical Kerr effect," *J. Magn. Magn. Mater.* Amsterdam, vol. 324, pp. 569-577, 2012.
- [13] R.A. Young (ed.), *The Rietveld Method: International Union of Crystallography Oxford University Press Oxford*, 1993.

TABLE I.
ANALYSIS OF CRYSTALLINE AND OXIDE PHASES IN NEAR-SURFACE REGION
OBTAINED BY RIETVELD ANALYSIS OF GIXRD MEASUREMENTS

T_a	vacuum			H_2		
	α -Fe(Si)	oxide	d Fe-grains	α -Fe(Si)	oxide	d Fe-grains
K	%	%	nm	%	%	nm
733	35	65	5	53	47	4
823	60	40	13	94	6	10

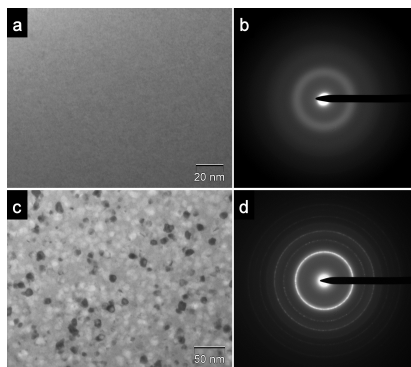


Fig. 1. TEM micrographs and SAD patterns of the FeSiNbCuB samples: (a, b) as-quenched state; (c, d) vacuum annealed 743 K.

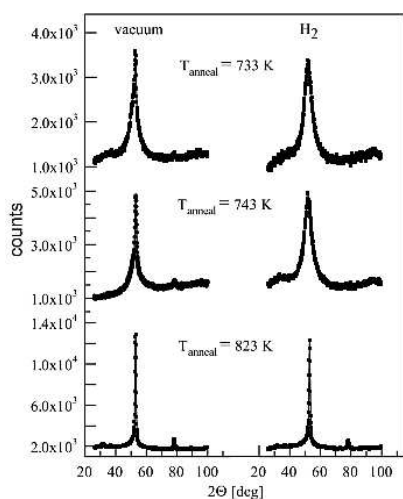


Fig. 2. X-ray diffraction spectra of vacuum and hydrogen annealed FeSiNbCuB samples.

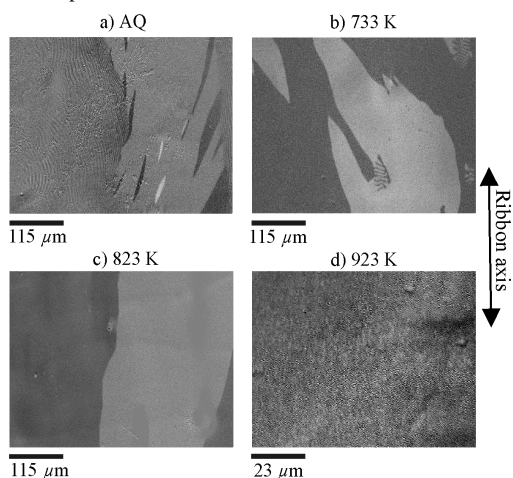


Fig. 5. MOKE domains images measured at remanence state for as-quenched (AQ) and vacuum-annealed FeSiNbCuB samples.

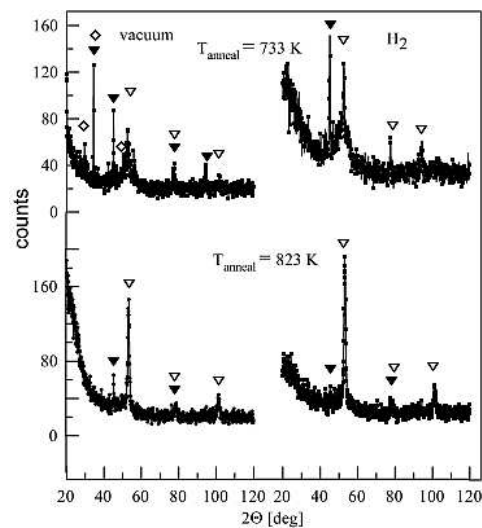


Fig. 3. GIXRD patterns obtained on vacuum (left column) and hydrogen (right column) annealed FeSiNbCuB samples at 733 K and 823 K; ∇ - α -Fe, \blacktriangledown - B_2O , and \diamond - $FeBO_3$.

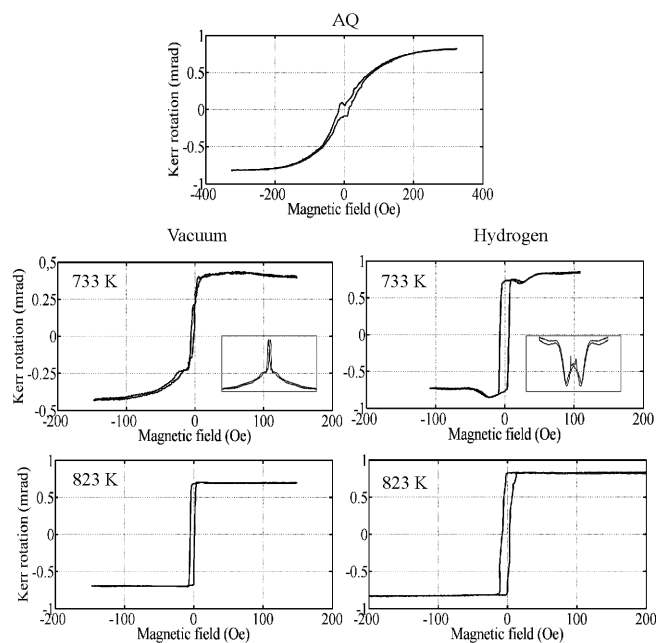


Fig. 4. MOKE hysteresis loops of FeSiNbCuB samples obtained at different annealing temperatures and atmospheres.